SELF-SIMILAR PHASE DYNAMICS OF BOUNDARY FRICTION

A.V. KHOMENKO, I.A. LYASHENKO, V.N. BORISYUK

Sumy State University
(2, Rymskyi-Korsakov Str., Sumy 40007, Ukraine; e-mail: khom@mss.sumdu.edu.ua, nabla04@ukr.net)

PACS 05.10.Gg, 05.30.Pr, 05.45.-a, 05.45.Tp, 07.05.Tp, 62.20.Fe, 62.20.Qp, 64.60.-i

The melting of an ultrathin lubricant film confined between two atomically flat solid surfaces has been studied. The phase diagram with the domains of sliding, dry, and intermittent (stick-slip) frictions has been constructed, by taking the additive noises of stress, strain, and temperature into account. The time series of stresses have been constructed for the parameters of all the modes within the Stratonovich calculus. In the case where the temperature noise intensity exceeds much more the intensities of stress and strain noises, the self-similar mode is established during the melting of a lubricant. The multifractality of the stress time series is shown to be provided by the power-law shape of the distribution function and by the presence of correlations in the system.

1. Introduction

Interest to sliding friction problems is caused by a large importance of their application in various scientific and engineering branches [1]. For last years, the intensive researches of atomically smooth surfaces separated by an ultrathin lubricant layer have been carried out. An anomalous behavior is inherent to such systems which may manifest itself in that there may exist several kinetic modes of friction. The transitions between these modes can be interpreted as phase transformations [2]. In this case, a liquid lubricant demonstrates the properties of a solid one [3]. A characteristic feature of such friction systems is an intermittent (stick-slip) motion typical of dry friction [4, 5]. Such a regime is observed, if the lubricant film thickness is narrower than that of three molecular layers, and it is explained as a periodic hardening induced by the squeezing action of the walls. The lubricant melts in the course of shearing, if the shear stresses σ that arise in the layer exceeds the critical value σ_c (the yield point) owing to the "shear melting" effect. Since the interest in such systems is enhanced, a number of models have been proposed to describe the indicated regularities. In particular, there are the deterministic mechanistic [4], stochastic mechanistic [6], thermodynamic [7], and rheological [8] models. In the framework of the latter model, the influence of additive noncorrelated noises of key parameters [9, 10], as well as correlated temperature fluctuations [11], on the melting has been studied. The features of the hysteretic behavior of a lubricant [12, 13] and its melting owing to the dissipative heating [14] have been considered.

It is worth noting that metallic monolayers deposited onto a mica surface can be used as lubricants in such systems [15]. In this case, a fractal morphology of the surface is formed in the boundary friction mode, as was shown in work [16]. Works [17–19] present the experimental data and theoretical models which evidence for a self-similar character of the stick-slip mode under dry friction. In particular, making use of a pin-on-disk tribometer for testing smooth friction surfaces of steel and aluminum, it was demonstrated [17] that the probability distribution of friction force jumps has a power-law character with the power exponent in the interval 2.2–5.4, whereas the power-law spectral density obeys the dependence $1/f^{-\alpha}$, where α falls in the interval from 1 to 2.6. The self-similar mode stimulated by temperature fluctuations was found in work [10] in the framework of rheological model and on the basis of a method described in work [20]. The present work aims at analyzing – in the framework of a rheological model – the time series for stresses that arise in the lubricant. The origin of multifractal behavior of the time series in the course of boundary friction has been revealed.

2. Basic Equations

In work [8], a system of kinetic equations was obtained on the basis of the rheological description of a viscoelastic medium characterized by a certain heat conductivity. This system determines a self-consistent behavior of shear stresses σ and strains ε, as well as the temperature T, in an ultrathin lubricant film in the process of friction between atomically smooth solid surfaces. In this approach, the main assumption was that the relaxation

equation for σ looks like

$$\tau_\sigma \dot{\sigma} = -\sigma + G\varepsilon, \tag{1}$$

where the first term on the right-hand side describes the Debye relaxation in the time interval $\tau_\sigma \equiv \eta_\sigma/G$, which is determined by the effective viscosity η_σ and the nonrelaxed shear modulus $G{\equiv}G(\omega)|_{\omega\to\infty}$ (ω is the circular frequency of a periodic external influence). By substituting $\partial\varepsilon/\partial t$ for ε/τ_σ, Eq. (1) is reduced to the Maxwell relation describing a viscoelastic medium which is widely used in the boundary friction theory [1]:

$$\frac{\partial\sigma}{\partial t} = -\frac{\sigma}{\tau_\sigma} + G\frac{\partial\varepsilon}{\partial t}. \tag{2}$$

In the stationary case, $\dot{\sigma} = 0$, and Eq. (1) gives rise to the Hooke law $\sigma = G\varepsilon$.

The relaxation behavior of a viscoelastic lubricant in the process of friction is described also by the Kelvin–Voigt equation [21]

$$\dot{\varepsilon} = -\varepsilon/\tau_\varepsilon + \sigma/\eta, \tag{3}$$

where τ_ε is the strain relaxation time, and η is the shear viscosity. The second term on the right-hand side describes a viscous liquid flow under the action of the stress shear component. In the stationary case, $\dot{\varepsilon} = 0$, and we have an expression similar to the Hooke law, $\sigma = G_\varepsilon\varepsilon$, where $G_\varepsilon{\equiv}\eta/\tau_\varepsilon{\equiv}G(\omega)|_{\omega\to 0}$ is the relaxed value of the shear modulus. Since Eq. (1) cannot be formally reduced to the Kelvin–Voigt equation (3) [21, 22], we supposed that the effective viscosity $\eta_\sigma{\equiv}\tau_\sigma G$ does not equal to the actual value of η. In addition, the simplest approximation for the temperature dependences should be adopted: $G_\varepsilon(T)$, $G(T)$, $\eta_\sigma(T) = \text{const}$, and

$$\eta = \frac{\eta_0}{T/T_c - 1}, \tag{4}$$

where η_0 is the characteristic value of shear viscosity η at $T = 2T_c$. It stems from the fact that the parameters G_ε, G, and η_σ depend very weakly on the temperature, whereas the actual viscosity η diverges, when the temperature decreases to its critical value T_c [23, 24]. The system of equations (1), (3), and (4) composes a new rheological model. The rheological properties of lubricant films are studied experimentally, which allows the phase diagram to be constructed [3].

According to the synergetic concept [25, 26], the system of equations (1) and (3), which include the order parameter σ, the conjugate field ε, and the control parameter T, should be appended by a kinetic equation for the temperature. Such an equation can be derived from the basic relations of elasticity theory [22]. We proceed from the expression that couples the time derivatives of the entropy S and the internal energy U with the equilibrium elastic stress σ_{el}:

$$T\frac{dS}{dt} = \frac{dU}{dt} - \sigma_{\text{el}}\frac{d\varepsilon}{dt}. \tag{5}$$

This is no more than the second principle of thermodynamics written down in the case of the mechanical loading of a solid (in the equilibrium, the heat variation is $\delta Q = TdS$). In the nonequilibrium case where the medium is heated non-uniformly, this relation looks like

$$-\text{div}\ \mathbf{q} = \frac{dU}{dt} - \sigma\frac{d\varepsilon}{dt}. \tag{6}$$

Here, the heat flux is determined by the Onsager relation

$$\mathbf{q} = -\kappa\nabla T, \tag{7}$$

where κ is the heat conduction, and the total stress $\sigma = \sigma_{\text{el}} + \sigma_{\text{v}}$ includes also the viscous component σ_{v}. Subtracting Eq. (6) from Eq. (5), taking into account the expression

$$\frac{dS}{dt} = \frac{\partial S}{\partial U}\left(\frac{\partial U}{dT}\right)_\varepsilon\frac{dT}{dt} + \frac{\partial S}{\partial U}\frac{\partial U}{\partial\varepsilon}\frac{d\varepsilon}{dt} + \left(\frac{\partial S}{\partial\varepsilon}\right)_U\frac{d\varepsilon}{dt} =$$

$$= \frac{\rho c_{\text{v}}}{T}\frac{dT}{dt} + \frac{1}{T}\frac{\partial U}{\partial\varepsilon}\frac{d\varepsilon}{dt} - \frac{\sigma_{\text{el}}}{T}\frac{d\varepsilon}{dt}, \tag{8}$$

and supposing that the lubricant layer and the atomically smooth friction surfaces have different temperatures – T and T_e, respectively – we obtain [8]

$$\rho c_{\text{v}}\dot{T} = \frac{\kappa}{l^2}(T_e - T) + \sigma_{\text{v}}\dot{\varepsilon} + T\frac{\partial\sigma_{\text{el}}}{\partial T}\dot{\varepsilon}. \tag{9}$$

In this equation, ρ is the lubricant density, c_{v} is its specific heat capacity, and l is the thickness of a lubricant layer or the distance between friction surfaces. Here, we also used the approximations $(\kappa/l^2)(T_e - T) \approx -\text{div}\ \mathbf{q}$ and $\partial U/\partial\varepsilon = \sigma_{\text{el}} - T\partial\sigma_{\text{el}}/\partial T$. The first term on the right-hand side of Eq. (9) describes the heat transfer from the lubricant layer to the friction surfaces, the second one makes allowance for the dissipative heating of the viscous liquid that flows under the stress action [27], and the third one stands for a heat source associated with the reversible mechanocalorific effect, for which we have $T(\partial\sigma_{\text{el}}/\partial T)\dot{\varepsilon} \approx \sigma_{\text{el}}\dot{\varepsilon}$ in the linear approximation. As a result, the heat conductivity equation looks like

$$\rho c_{\text{v}}\dot{T} = \frac{\kappa}{l^2}(T_e - T) + \sigma\dot{\varepsilon}. \tag{10}$$

Now, the system of Eqs. (1), (3), and (10) is complete and is characterized by three degrees of freedom, which allows one to describe a non-trivial behavior of a thin lubricant film at its melting [25].

The reduction of Eqs. (1), (3), and (10) to the dimensionless form allows one to decrease the number of constants under consideration. We now introduce the following measurement units for the variables σ, ε, and T:

$$\sigma_s = \left(\frac{\rho c_{\rm v}\eta_0 T_c}{\tau_T}\right)^{1/2}, \quad \varepsilon_s = \frac{\sigma_s}{G_0}, \quad T_c, \tag{11}$$

where $G_0 \equiv \eta_0/\tau_\varepsilon$ is the characteristic value of the shear modulus, and $\tau_T \equiv \rho l^2 c_{\rm v}/\kappa$ is the heat conduction duration. Then, after the substitution of the derivative $\dot{\varepsilon}$ from formula (3) into Eq. (10), Eqs. (1), (3), and (10) acquire the form

$$\tau_\sigma \dot{\sigma} = -\sigma + g\varepsilon + \sqrt{I_\sigma}\xi_1(t), \tag{12}$$

$$\tau_\varepsilon \dot{\varepsilon} = -\varepsilon + (T-1)\sigma + \sqrt{I_\varepsilon}\xi_2(t), \tag{13}$$

$$\tau_T \dot{T} = (T_e - T) - \sigma\varepsilon + \sigma^2 + \sqrt{I_T}\xi_3(t), \tag{14}$$

where the constant $g = G/G_0 < 1$. The equations obtained formally coincide with the Lorenz synergetic system [28], in which the shear stresses play the role of order parameter, the conjugate field is reduced to a shear strain, and the temperature is a control parameter. Such a system is known to be used for the description of both thermodynamic [25] and kinetic [26] phase transformations.

In Eqs. (12)–(14), the δ-correlated Gaussian stochastic sources $\xi_i(t)$ with the intensities I_σ, I_ε, and I_T, measured in the units of σ_s^2, $\varepsilon_s^2\tau_\varepsilon^{-2}$, and $(T_c\kappa/l)^2$, respectively, were introduced in order to take the influence of key parameter fluctuations into account [9]. The moments of the functions $\xi_i(t)$ are defined as follows[1]:

$$\langle \xi_i(t)\rangle = 0, \quad \langle \xi_i(t)\xi_j(t')\rangle = 2\delta_{ij}\delta(t-t'). \tag{15}$$

In work [8], the lubricant melting was interpreted as a result of the spontaneous emergence of shear stresses, when the friction surfaces became heated above the critical temperature $T_{c0} = 1 + g^{-1}$. The primary origin of the self-organization process is a positive feedback of T and σ with ε [see Eq. (13)] related to the temperature dependence of the shear viscosity (4), which results in the divergence of the latter. On the other hand, the negative feedback of σ and ε with T in Eq. (14) plays an important role, because it provides the system stability.

In accordance with such an approach, the lubricant is a very viscous liquid which behaves as an amorphous solid; it has a large effective viscosity, being still characterized by a certain fluidity threshold [3, 21]. Its solid-like state corresponds to shear stresses $\sigma = 0$, because Eq. (12) drops out of consideration at that ($\dot{\sigma} = 0$). Equation (13) which contains viscous stresses can be reduced to the Debye law describing the fast relaxation of a shear strain in the microscopic time interval $\tau_\varepsilon \approx a/c \sim 10^{-12}$ s, where $a \sim 1$ nm is the lattice constant or the intermolecular distance, and $c \sim 10^3$ m/s is the speed of sound. In this case, the heat equation (14) acquires the simplest form for the temperature relaxation to T_e, because the terms that correspond to the dissipative heating and the mechanocalorific effect in a viscous liquid disappear from it.

At nonzero stress values σ, Eqs. (12)–(14) describe the properties indicated above as for the lubricant in a liquid-like state. Such a behavior strongly differs from that of bulk lubricants and requires a detailed explanation. According to Eq. (13), the appearance of viscous stresses $\sigma_{\rm v}$ results in a plastic flow of the liquid-like lubricant with the velocity $V = l\partial\varepsilon/\partial t$. In particular, in the case of surface force apparatus [29, 30], the effective amplitude of deformation $\varepsilon = x_{\max}/l$ in Eqs. (12)–(14) is determined through the ratio between the deformation amplitude (deviation) $x_{\max}$ and the lubricant thickness l. The effective shear velocity $\dot{\varepsilon} = \varepsilon\omega = V/l = \varepsilon/\tau_\sigma$ is a product of the strain ε and the oscillation frequency ω.

In work [7], the plastic flow was demonstrated to be realized in a lubricant layer, provided that elastic stresses are available in the latter. In this case, the shear stresses reduce the shear modulus of the lubricant [31]. In accordance with the results of work [32], the increase of viscous stresses

$$\sigma_{\rm v} = \frac{F_{\rm v}}{A} \tag{16}$$

in the boundary friction mode is accompanied by an increase of the viscous friction force:

$$F_{\rm v} = \frac{\eta_{\rm eff} V A}{l}, \tag{17}$$

where $\eta_{\rm eff}$ is the effective viscosity which does not coincide with the actual viscosity and can be found only experimentally [32], and A is the contact area. Combining Eqs. (16) and (17), we obtain an expression for the

[1] The factor of 2 was chosen in order to make the corresponding Fokker–Planck equation (FPE) look simpler.

velocity in terms of stresses:

$$V = \frac{\sigma_{\rm v} l}{\eta_{\rm eff}}. \tag{18}$$

Hence, the growth of shear stresses gives rise to an increase of the relative velocity of motion of contacting surfaces, and the lubricant melts.

Moreover, according to the results of work [5], in the absence of a shear deformation, the heat-induced root-mean-square deviation of molecules (atoms) is determined by the equality $\langle u^2\rangle = T/(Ga)$. The average deviation, which the shearing is responsible for, is determined from the relation $\langle u^2\rangle = \sigma^2 a^2/G^2$. The total root-mean-square deviation is equal to the sum of those expressions, provided that thermal fluctuations and stresses are not interconnected. This means that the lubricant melting originates from both heating and the influence of stresses created by the solid surfaces in the course of friction. The latter conclusion agrees with the consideration of an unstable solid-like state in the framework of a model, where the shear dynamic melting occurs in the absence of thermal fluctuations. Therefore, the strain fluctuations associated with stresses and thermal fluctuations have to be analyzed separately. We assume that the lubricant film becomes more liquid-like and the friction force decreases with the temperature growth due to a reduction of the activation energy of molecular jumps.

3. Dynamic Phase Diagram

To analyze the system further, we will operate in the framework of a method described in work [20]. Using the adiabatic approximation $\tau_\sigma \gg \tau_\varepsilon, \tau_T$ [8, 10], we may put $\tau_\varepsilon\dot{\varepsilon} \approx 0$ and $\tau_T\dot{T} \approx 0$ in Eqs. (13) and (14). Then, these equations give rise to the dependences

$$\varepsilon(t) = \bar{\varepsilon} + \tilde{\varepsilon}\xi_4(t), \quad T(t) = \bar{T} + \widetilde{T}\xi_5(t), \tag{19}$$

$$\bar{\varepsilon} \equiv \sigma\left(T_e - 1 + \sigma^2\right) d(\sigma),\ \tilde{\varepsilon} \equiv \sqrt{I_\varepsilon + I_T\sigma^2}\ d(\sigma),$$

$$\bar{T} \equiv \left(T_e + 2\sigma^2\right) d(\sigma),\ \widetilde{T} \equiv \sqrt{I_T + I_\varepsilon\sigma^2}\ d(\sigma), \tag{20}$$

where $d(\sigma) \equiv (1+\sigma^2)^{-1}$. Here, the deterministic components can be reduced to the equalities obtained in work [8]. At the same time, the fluctuation components originate from the known property of dispersion additivity for Gaussian random variables [33]. Hence, the synergetic principle of subordination [25, 26] transforms the additive noises of strain ε and temperature T into multiplicative ones. As a result, expressions (12), (19), and (20) lead to the Langevin equation [9, 10, 14]

$$\dot{\sigma} = f(\sigma) + \sqrt{I(\sigma)}\ \xi(t), \tag{21}$$

where the time t is measured in stress relaxation time units τ_σ.

The generalized force $f(\sigma)$ and the effective noise intensity $I(\sigma)$ are given by the equalities [9]

$$f(\sigma) \equiv -\sigma + g\sigma\left[1 - (2 - T_e)(1+\sigma^2)^{-1}\right],$$

$$I(\sigma) \equiv I_\sigma + g^2(I_\varepsilon + I_T\sigma^2)(1+\sigma^2)^{-2}. \tag{22}$$

To prevent any misunderstanding, it should be noted that a direct substitution of Eqs. (19), and (20) into Eq. (12) generates a stochastic additive

$$\left[I_\sigma^{1/2} + g\left(I_\varepsilon^{1/2} + I_T^{1/2}\sigma\right)\left(1+\sigma^2\right)^{-1}\right]\xi(t), \tag{23}$$

the squared amplitude of which differs from the effective noise intensity (22). Moreover, the direct use of the adiabatic approximation in Eqs. (13) and (14) results in fluctuation terms of the form $\widetilde{\varepsilon} \equiv (I_\varepsilon^{1/2} + I_T^{1/2}\sigma)d(\sigma)$ and $\widetilde{T} \equiv (I_T^{1/2} - I_\varepsilon^{1/2}\sigma)d(\sigma)$ in dependences (19). The latter fluctuation term is evidently unphysical, because the effective temperature noise $\widetilde{T}$ disappears completely at stresses $\sigma = \sqrt{I_T/I_\varepsilon}$. A formal reason for such a contradiction is the fact that the conventional methods of analysis cannot be applied to the Langevin equation [33].

For a further consideration, let us multiply Eq. (21) by dt to obtain the differential Langevin relation

$$d\sigma = f(\sigma)dt + \sqrt{I(\sigma)}dW(t), \tag{24}$$

where $dW(t) = W(t+dt) - W(t) \equiv \xi(t)dt$ is a Wiener process with the properties [35]

$$\langle dW(t)\rangle = 0; \quad \langle (dW(t))^2\rangle = 2dt. \tag{25}$$

In the general case, a number of FPE forms can correspond to Eq. (24). In works [10, 14], the FPE in the Itô form was used, because it has a simpler form. In what follows, we proceed from the Stratonovich calculus, since it allows the memory effects, which occur at the melting of ultrathin lubricant films owing to their small dimensions, to be taken into consideration automatically. The corresponding FPE, which makes allowance for Eq. (25), reads

$$\frac{\partial P(\sigma,t)}{\partial t} = -\frac{\partial}{\partial\sigma}\left[f(\sigma)P(\sigma,t)\right] +$$

$$+\frac{\partial}{\partial\sigma}\left[\sqrt{I(\sigma)}\frac{\partial}{\partial\sigma}\sqrt{I(\sigma)}P(\sigma,t)\right]. \qquad (26)$$

In due course, the distribution of solutions of Eq. (24) becomes stationary, and its explicit form can be found from Eq. (26), where $\partial P(\sigma,t)/\partial t = 0$ should be put. We obtain

$$P(\sigma) = \mathcal{Z}^{-1}\exp\{-U(\sigma)\}, \qquad (27)$$

where the effective potential is determined by the equality

$$U(\sigma) = \frac{1}{2}\ln I(\sigma) - \int\limits_0^\sigma \frac{f(\sigma')}{I(\sigma')}d\sigma'. \qquad (28)$$

The extremum points of distribution (27) are defined by the condition $dU/d\sigma \equiv dI/d\sigma - 2f = 0$ or, in the explicit form, by the equation

$$(1-g)x^3 + g(2-T_e)x^2 - g^2 I_T x + 2g^2(I_T - I_\varepsilon) = 0, \qquad (29)$$

where $x \equiv 1+\sigma^2$. Expression (29) differs from its counterpart obtained in work [9, 10]. However, if the noise intensities I_T and I_ε in Eq. (29) become two times larger, the discrepancy disappears. Therefore, the results of the further analysis, which is based on studying the extrema of distribution functions (plotting the phase diagram and the interpretation of stationary states) making use of the Stratonovich calculus, coincide with those obtained in the framework of the Itô approach [10]. However, potential (28) cannot be reduced to that obtained earlier [10], if a simple renormalization of noise intensities is carried out, because those two potentials differ from each other by their first terms only (the presence of the coefficient of 1/2). Therefore, the time series for stresses are also different. Since the presented work aims at studying the features of the stress evolution in time, we use the Stratonovich calculus.

At a fixed intensity I_ε, the phase diagram looks like that depicted in Fig. 1,*a*, and, at a fixed intensity I_T, like that depicted in Fig. 1,*b*. Curves *1′* and *2′* on the diagrams correspond to the system stability thresholds. The straight line *1′* is defined by the equality

$$T_e = 1 + g^{-1} + g(I_T - 2I_\varepsilon) \qquad (30)$$

which follows from Eq. (29) and denotes the existence threshold for the nonzero stationary solution $\sigma_0 = 0$. Below this straight line, the maximum of $P(\sigma)$ is always realized at $\sigma = 0$, and there is no maximum above it. The diagram demonstrates three regions which

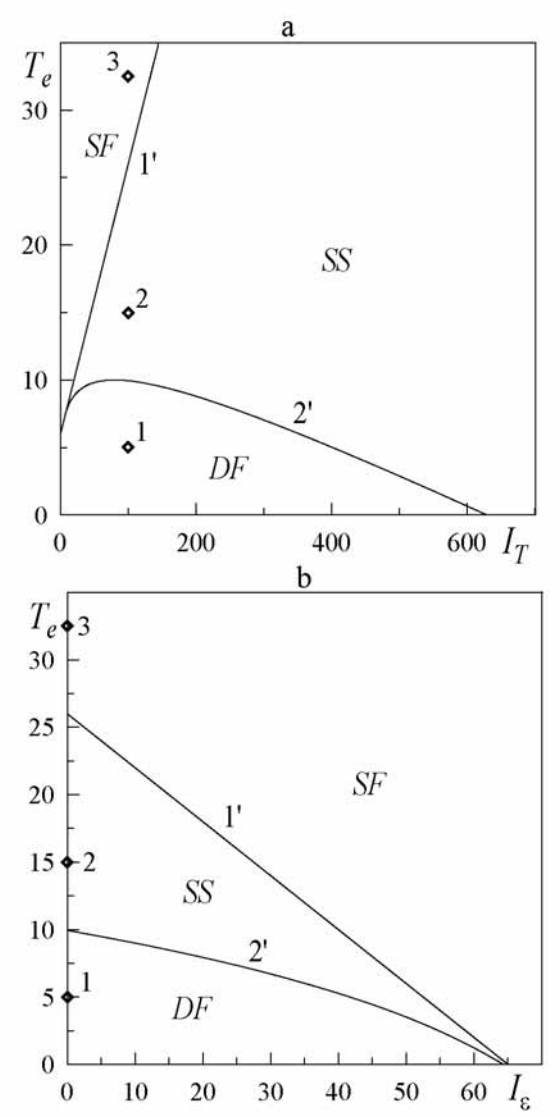

Fig. 1. Phase diagrams with the regions of liquid (SF), dry (DF), and stick-slip (SS) frictions at (a) $I_\varepsilon = 0$ and (b) $I_T = 100$. Parameter $g = 0.2$

correspond to different friction modes. Actually, both panels are plane cross-sections of the three-dimensional phase diagram in the $T_e - I_\varepsilon - I_T$ coordinates. Therefore, points 1 to 3 on both diagrams, which were selected for further analysis, were chosen at the intersection of both secant planes in such a manner that they correspond to identical parameters of the system.

Figure 2 illustrates non-normalized probability distributions (27), which correspond to points in Fig. 1. Point 1 is located in the dry friction region DF of the

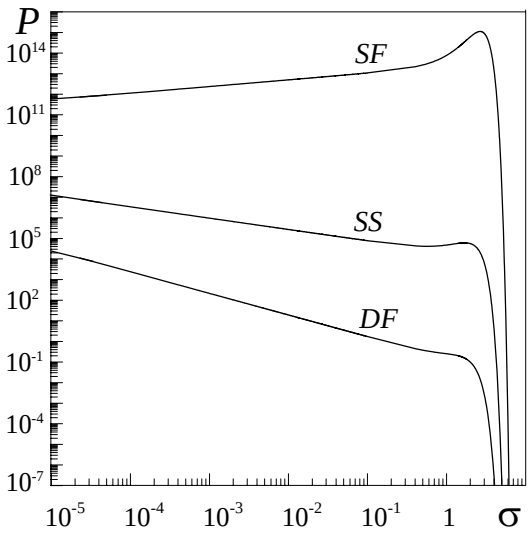

Fig. 2. Distribution function (27) at $I_\sigma = 10^{-20}$, $I_\varepsilon = 0$, and $I_T = 100$, in the modes denoted by points in Fig. 1: *1* – $T_e = 5$ (DF), *2* – $T_e = 15$ (SS), *3* – $T_e = 32.5$ (SF)

phase diagram; therefore, a single maximum of the distribution function $\sigma_0 = 0$ is observed.

The biphase region SS of the diagram is characterized by the coexistence of $P(\sigma)$-distribution maxima at the zero and nonzero stress values (point 2). Point 3 is located in the region, where a single maximum of the probability distribution at $\sigma_0 \neq 0$ is observed, which corresponds to the liquid friction mode or sliding.

The dependences $P(\sigma)$ in Fig. 2 are plotted in the log-log scale. The figure shows that the distributions for curves DF and SS acquire a decaying power-law dependence. This mode corresponds to such values of $\sigma \ll 1$ and $I_\sigma, I_\varepsilon \ll I_T$, at which Eq. (27) can be reduced to the form

$$P(\sigma) = \sigma^{-1}\mathcal{P}(\sigma), \tag{31}$$

where the function $\mathcal{P}(\sigma)$ is defined by the expression

$$\mathcal{P}(\sigma) = \mathcal{Z}^{-1} g^{-1} I_T^{-1/2}(1+\sigma^2)\times$$

$$\times \exp\left\{ I_T^{-1} g^{-1}\left[\frac{\sigma^4}{4}(1-g^{-1})+\right.\right.$$

$$\left.\left.+(T_e - 1 - g^{-1})\ln\sigma + \sigma^2\left(\frac{T_e}{2} - g^{-1}\right)\right]\right\}. \tag{32}$$

Self-similar systems are known to be described by a homogeneous distribution function [34]. Distribution (31) is homogeneous in the case where function (32) is constant. At small stress values, the preexponential multiplier $1 + \sigma^2 \to 1$. Let us analyze the terms in the exponent which contribute to the distribution. The first term, owing to the fourth power, makes an insignificant contribution, when the stresses are low, and, since $g < 1$, it is always negative, which means that the distribution has an exponentially decaying character at high stresses. The second and third terms also grow at high temperatures, if the stresses increase. Therefore, as is seen from Fig. 2, the power-law asymptotics $P(\sigma) \propto \sigma^{-1}$ is not observed in mode SF, and the probability becomes a growing function at small σ-values. Thus, the available self-similar behavior should be expected at temperatures, for which the second and third terms decrease in the range $\sigma < 1$ with the stress growth, i.e. at $T_e < 1 + g^{-1}$.

The Stratonovich calculus revealed a first considerable difference in comparison with the Itô approach: the distribution index is equal to -1 in Eq. (31) and to -2 in the relevant expression of work [10].

4. Time Series for Stresses

In order to solve Eq. (24) numerically, let us take advantage of the Euler method. However, since this equation is a Stratonovich stochastic differential equation (SDE) in our case, the iteration procedure differs from that used in work [14]. To use an ordinary iteration procedure, a transformation from the Stratonovich SDE to an equivalent Itô SDE is necessary. Equation (24), together with Eq. (25), gives rise to the Itô SDE in the form [35, 36]

$$d\sigma = \left[f(\sigma) + \sqrt{I(\sigma)}\frac{\partial}{\partial\sigma}\sqrt{I(\sigma)}\right]dt + \sqrt{I(\sigma)}dW(t). \tag{33}$$

Taking the definition of a discrete analog of the random force differential $dW(t) \equiv \sqrt{\Delta t}W_i$ and Eq. (22) into account, we obtain the iterative procedure for the solution of Eq. (33):

$$\sigma_{i+1} = \sigma_i + \left(f(\sigma_i) + \frac{g^2\sigma_i[I_T(1-\sigma_i^2) - 2I_\varepsilon]}{(1+\sigma_i^2)^3}\right)\Delta t +$$

$$+\sqrt{I(\sigma_i)\Delta t}W_i. \tag{34}$$

This equation is solved in the time interval $t \in [0, T]$. Provided that the number of iterations N (the number of points in the time series) is given, the time increment is determined as $\Delta t = T/N$. The force W_i is characterized by the following properties (cf. with Eq. (25)):

$$\langle W_i\rangle = 0, \quad \langle W_i W_{i'}\rangle = 0, \quad \langle W_i^2\rangle \to 2. \tag{35}$$

The Box–Muller model [37] allows a stochastic force that has white-noise properties to be presented adequately:

$$W_i = \sqrt{\mu^2}\sqrt{-2\ln r_1}\cos(2\pi r_2), \quad r_n \in (0,1]. \tag{36}$$

Here, in accordance with Eqs. (35), the dispersion $\mu^2 = 2$, and W_i is an absolutely random number, the properties of which are characterized by Eqs. (35). Pseudorandom numbers r_1 and r_2 have uniform distributions.

Effective potential (28) possesses minima at both positive and negative stress values σ. Therefore, when Eq. (33) is solved numerically, transitions of the system between states that correspond to the minima indicated are possible due to fluctuations. By examining the motion of the upper surface that moves unidirectionally, we will analyze the behavior of $|\sigma|(t)$ in what follows. Typical realizations of $|\sigma|(t)$ for the modes under consideration are exhibited in Fig. 3.

In the case of dry friction (mode DF), the dependence $|\sigma|(t)$ demonstrates long-term sections, where stresses are close to zero and which are separated by narrow peaks. In the inset, the same dependence $|\sigma|(t)$ is shown scaled-up. One can see that the behavior does no change its character at scaling, i.e. it is self-similar. In the parameter range of stick-slip friction (mode SS), stochastic transitions occur between the zero and nonzero stress values σ. In the liquid friction mode (SF), stresses fluctuate near a nonzero average value.

5. Multifractal Fluctuation Analysis of Self-Similar Time Series

The multifractal fluctuation analysis allows the basic multifractal characteristics [38] used for the description of self-similar systems to be calculated numerically. Such an analysis is carried out in the framework of a method that was suggested for the first time in work [39]. For self-similar time series, the essence of the method consists in the numerical calculation of the fluctuation function $F_q(s)$ associated with the scale parameter s by the scaling relation [39]

$$F_q \sim s^{h(q)}, \tag{37}$$

where $h(q)$ is the generalized Hurst exponent depending on the parameter q, which can accept any real value (it is worth noting that $h(q)$ at $q = 2$ corresponds to the classical Hurst exponent H [40]). Hence, the function $h(q)$ is calculated as a slope of $F_q(s)$ in logarithmic coordinates, where it should be linear.

It is more convenient to describe the self-similar properties of time series by making use of a multifractal spectrum function $f(\alpha)$ [38, 39],

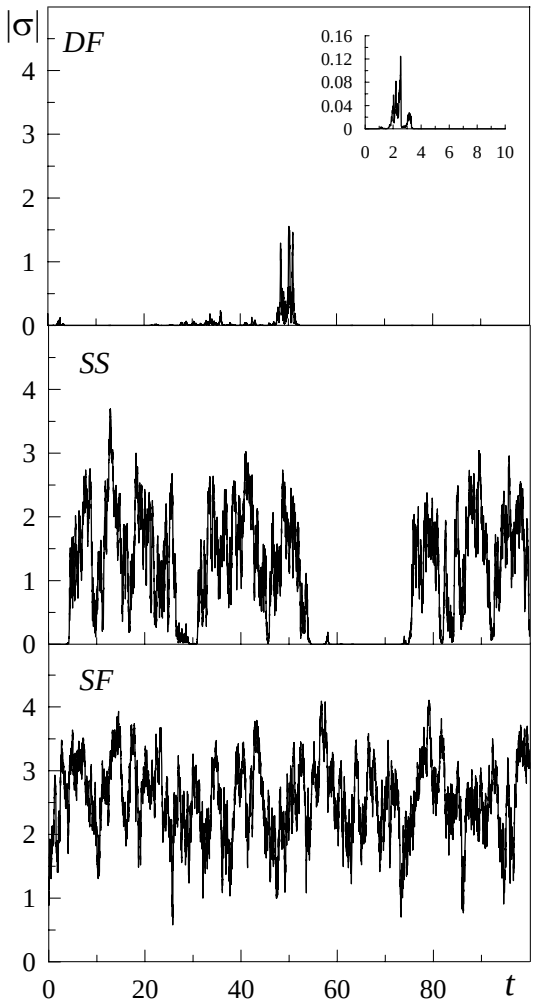

Fig. 3. Time series for stresses $|\sigma|(t)$ obtained by iterative procedure (34) at $N = 10^4$, $t = 100$, and $\Delta t = 0.01$. The indicated modes correspond to the points on the phase diagram (Fig. 1)

$$f(\alpha) = q[\alpha - h(q)] + 1, \tag{38}$$

where α is the Hölder exponent which is calculated by the formula

$$\alpha = h(q) + q\frac{dh(q)}{dq}. \tag{39}$$

The form of the indicated dependences characterizes the time series properties. For instance, a constant value, $h(q) = \text{const}$, corresponds to a simple monofractal series. A reduction of the function $h(q)$ with the growth of q is inherent to more complicated multifractal series which are characterized by a spectrum of fractal dimensions. In

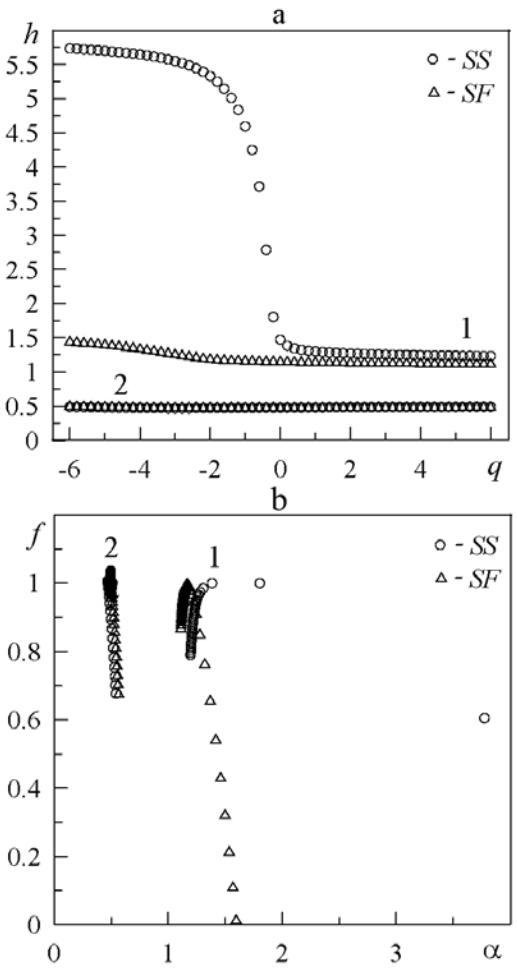

Fig. 4. Multifractal characteristics $h(q)$ and $f(\alpha)$ corresponding to the parameters of the series shown in Fig. 3. The group of curves *1* corresponds to series obtained directly by the iteration procedure (34), whereas the group of curves *2* to the same "shuffled" series

this case, there is a single value of the Hölder exponent α for monofractal objects, so that the dependence $f(\alpha)$ is the delta-function. In the case of multifractal series, a spectrum of $f(\alpha)$-values is realized.

Two reasons are adopted to be responsible for the multifractal properties of time series in the general case. First, the multifractality can be caused by a wide probability distribution function for elements in the series. Second, it can be a result of time correlations between the series terms. If the series terms are shuffled, so that they become rearranged in a random order, the multifractal properties will not be violated for the series of the first type. But, in the second case, such a regrouping of terms will destroy available correlations. Since the "origin" of multifractality disappears at that, a strongly correlated complicated series transforms into a simpler monofractal one. In the case where both origins of multifractal properties are inherent to a time series, the corresponding "shuffled" series will be characterized by weaker self-similar properties and, respectively, by a narrower spectrum of fractal dimensions $f(\alpha)$ than the "original" one [39]. Therefore, by studying the original and corresponding shuffled time series by the method of work [39], one can reveal the presence of time correlations and the origin of self-similar properties.

Taking advantage of the method described above, let us analyze the time series for stresses $|\sigma|(t)$ depicted in Fig. 3. For this purpose, let us calculate the dependences $h(q)$ and $f(\alpha)$ for the parameter values $N = 10^5$, $t = 5 \times 10^3$, and $\Delta t = 0.05$[2]. On the basis of the dependences shown in Fig. 4, it is evident that multifractal properties manifest themselves most pronouncedly in the series that corresponds to mode SS. The series that corresponds to mode SF is characterized by a weak dependence of the parameter h on q; however, this series is also multifractal.

The well-pronounced multifractality for mode SS is explained by the fact that, in this mode, the distribution function has a decaying power-law dependence at small stresses, which corresponds to self-similar systems. In mode SF, the multifractality is expressed weaker, because the specified $P(\sigma)$-feature is not realized. On the basis of the given description, a conclusion can be drawn that a pronounced multifractality originates from the power-law dependence of the distribution function. To trace whether the power-law form of $P(\sigma)$ is a sufficient condition for the multifractality to exist, it is necessary to "shuffle" the studied time series and to find the fractal characteristics of the system once more. At the "shuffling" of the series, the correlations disappeared; however, since the characteristic values of series terms do not change at a random rearrangement of the latter, the form of the distribution function remains intact.

The group of curves *2* in Fig. 4 corresponds to the analysis of time series after the arrangement of their elements. One can see that the dependence $h(q)$ is the same straight line $h = 0.5$ for the parameters of all series, and

[2] Further calculations are not presented for mode DF, since the method produces a substantial error for series similar to the DF one exhibited in Fig. 3 (sparse peaks separated by values close to zero). In particular, the function $h(q)$ becomes growing in some q-range, which is unphysical. However, even in this case, one can assert unambiguously that the series for mode DF is multifractal, because $h(q)$ falls down at large q-values.

the dependence $f(\alpha)$ is a delta-like function with a small width. Such features correspond to monofractal series with the value $h = 0.5$ being typical of series without correlations. Thus, for the system under investigation, the self-similar properties of the corresponding time series for stresses are associated with a power-law form of the distribution function, as well as with correlations. If the power-law form of the dependence $P(\sigma)$ is violated or the correlations are absent, the multifractality disappears.

6. Conclusions

The melting of an ultrathin lubricant film has been studied in the framework of a rheological model which is parametrized by shear stresses and strains, as well as the temperature. Three modes of the lubricant behavior have been found, and they are characterized by different sets of maxima for the distribution functions of stresses. By analyzing the Langevin equation in the framework of a numerical simulation approach, the time series for stresses have been constructed for each mode. The basic multifractal characteristics have been calculated, and the origin of self-similar properties has been found to be associated with correlations in the time series and the power-law dependence of the distribution function. The power-law distribution is observed in the case where the temperature noise intensity is much higher than the intensities of stress and strain noises. The results of our consideration of the time series at various parameter values testify that the series are multifractal for all friction modes. It is probable that the multifractality of the series that corresponds to mode SF is caused by the growing power-law dependence $P(\sigma)$. In this case, since the realization probability for stresses corresponding to the power-law form of $P(\sigma)$ is low, a weakly pronounced multifractality is observed.

We express our gratitude to the State Foundation of Fundamental Researches of Ukraine (Grants Ф25/668-2007 and Ф25/97-2008) for the support of the work.

1. B.N.J. Persson, *Sliding Friction. Physical Principles and Applications* (Springer, Berlin, 1998).
2. E.A. Brener and V.I. Marchenko, JETP Lett. **76**, 211 (2002).
3. H. Yoshizawa, Y.-L. Chen, and J. Israelachvili, J. Phys. Chem. **97**, 4128 (1993); H. Yoshizawa and J. Israelachvili, J. Phys. Chem. **97**, 11300 (1993).
4. J.M. Carlson and A.A. Batista, Phys. Rev. E **53**, 4153 (1996).
5. I.S. Aranson, L.S. Tsimring, and V.M. Vinokur, Phys. Rev. B **65**, 125402 (2002).
6. A.E. Filippov, J. Klafter, and M. Urbakh, Phys. Rev. Lett. **92**, 135503 (2004).
7. V.L. Popov, Tech. Phys. **46**, 605 (2001).
8. A.V. Khomenko and O.V. Yushchenko, Phys. Rev. E **68**, 036110 (2003).
9. A.V. Khomenko, Phys. Lett. A **329**, 140 (2004).
10. A.V. Khomenko and I.A. Lyashenko, Tech. Phys. **50**, 1408 (2005).
11. A.V. Khomenko and I.A. Lyashenko, Fluct. Noise Lett. **7**, L111 (2007).
12. A.V. Khomenko and I.A. Lyashenko, Physics of the Solid State **49**, 936 (2007).
13. A.V. Khomenko and I.A. Lyashenko, Phys. Lett. A **366**, 165 (2007).
14. A.V. Khomenko and I.A. Lyashenko, Tech. Phys. **52**, 1239 (2007).
15. J.L. Parker and H.K. Christenson, J. Chem. Phys. **88**, 8013 (1988).
16. O.S. Kiselevskii and V.P. Kazachenko, J. Friction and Wear **27**, 59 (2006).
17. S.V. Buldyrev, J. Ferrante, and F.R. Zypman, Phys. Rev. E **74**, 066110 (2006).
18. F. Slanina, Phys. Rev. E **59**, 3947 (1999).
19. D.P. Vallette and J.P. Gollub, Phys. Rev. E **47**, 820 (1993).
20. E.A. Toropov and D.O. Kharchenko, Izv. Vyssh. Ucheb. Zaved. Fiz. **4**, 75 (1996).
21. *Rheology,* edited by F.R. Eirich (Academic Press, New York, 1960).
22. L.D. Landau and E.M. Lifshitz, *Theory of Elasticity* (Pergamon, New York, 1959).
23. A. Havranek and M. Marvan, Ferroelectrics **176**, 25 (1996).
24. A.I. Olemskoi and E.A. Toropov, Fiz. Met. Metalloved. **9**, 5 (1991).
25. H. Haken, *Advanced Synergetics: Instability Hierarchies of Self-Organizing Systems and Devices* (Springer, New York, 1993).
26. A.I. Olemskoi and A.V. Khomenko, JETP **83**(6), 1180 (1996).
27. A.I. Olemskoi and A.V. Khomenko, Tech. Phys. **45**, 672 (2000); **45**, 677 (2000).
28. E.N. Lorenz, J. Atmos. Sci. **20**, 130 (1963).
29. J. Israelachvili, Surf. Sci. Rep. **14**, 109 (1992).
30. A.L. Demirel and S. Granick, J. Chem. Phys. **109**, 6889 (1998).

31. G. Reiter, A.L. Demirel, J. Peanasky *et al.*, in *Physics of Sliding Friction,* edited by B.N.J. Persson and E. Tosatti (Kluwer, Dordrecht, 1995), p. 119.

32. G. Luengo, J. Israelachvili, and S. Granick, Wear **200**, 328 (1996).

33. H. Risken, *The Fokker–Planck Equation* (Springer, Berlin, 1989).

34. D.J. Amit, *Field Theory, the Renormalization Group, and Critical Phenomena* (McGraw-Hill, New York, 1978).

35. C.W. Gardiner, *Handbook of Stochastic Methods for Physics, Chemistry and the Natural Sciences* (Springer, Berlin, 1985).

36. V. Horsthemke and R. Lefever, *Noise-Induced Transitions* (Springer, Berlin, 1984).

37. W.H. Press, B.P. Flannery, W.T. Vetterling, and S.A. Teukolsky, *Numerical Recipes in C: the Art of Scientific Computing* (Cambridge University Press, New York, 2002).

38. A.I. Olemskoi, in *Physics Reviews, Vol. 18,* edited by I.M. Khalatnikov (Gordon and Breach, London, 1996), part 1, p. 1.

39. J.W. Kantellhardt, S.A. Zschiegner, E. Koscielny-Bunde *et al.*, Physica A **316**, 87 (2002).

40. J. Feder, *Fractals* (Plenum Press, New York, 1988).

Received 29.12.08.
Translated from Ukrainian by O.I. Voitenko

САМОПОДІБНА ФАЗОВА ДИНАМІКА МЕЖОВОГО ТЕРТЯ

О.В. Хоменко, Я.О. Ляшенко, В.М. Борисюк

Р е з ю м е

Досліджено плавлення ультратонкої плівки мастила, затиснутої між двома атомарно-гладкими твердими поверхнями. При врахуванні адитивних шумів напружень, деформації і температури побудовано фазову діаграму з областями рідинного, сухого і переривчастого тертя. Для параметрів усіх режимів у межах числення Стратоновича побудовано часові ряди напружень. У випадку, коли інтенсивність шуму температури набагато перевищує інтенсивності шумів напружень і деформації, встановлюється самоподібний режим при плавленні мастила. Показано, що мультифрактальність часових рядів напружень забезпечується степеневим виглядом функції розподілу і наявністю в системі кореляцій.